DIFFRACTION TRAVELTIME APPROXIMATION FOR GENERAL ANISOTROPIC MEDIA

A. Pronevich, S. Dell, B. Kashtan, D. Gajewski

email: *annpronevich@gmail.com*

keywords: *anisotropy, diffraction, traveltime*

ABSTRACT

In this paper we derive an approximation for the diffraction response for a general 2D anisotropic medium. Our traveltime expression is formulated as a double-square-root equation that allows us to accurately and reliably describe diffraction traveltimes. The diffraction response depends on the ray velocity which varies with angle and thus offset. To eliminate the angle dependency, we suggest to expand the ray velocity in a Taylor series around a reference ray. We choose the fastest ray of the diffraction response, i.e., the ray corresponding to the diffraction apex as the reference ray in this study. Moreover in an anisotropic medium, the location of the diffraction apex may be shifted with respect to the surface projection of the diffractor location. To properly approximate the diffraction response we consider this shift. The proposed approximation depends on four independent parameters: emergence angle of the fastest ray, ray velocity along this ray, and first and second-order derivatives of the ray velocity with respect to the ray angle. We also establish relations between anisotropy parameters and Thomsen parameters for homogeneous media with polar anisotropy.

INTRODUCTION

Diffractions carry detailed information on structural features of the subsurface which are of great interest in seismic exploration. This information can be used, e.g., for high-resolution imaging (see, e.g., Khaidukov et al., 2004; Dell and Gajewski, 2011) or migration velocity analysis (see, e.g., Reshef and Landa, 2009; Dell and Gajewski, 2012). However, until now only isotropic media have been considered in diffraction imaging. The frequently used approximation for diffraction traveltimes in heterogeneous media implements a conventional double-square-root (DSR) equation which is valid for media with moderate lateral velocity variations (Landa and Keydar, 1997). In the DSR approximation the surface projection of the diffractor coincides with the surface location of the fastest ray. Unfortunately, this simplification fails for many geological models due to seismic anisotropy. Figure 1(a) displays a top view of the diffraction response in an isotropic medium for a model shown in Figure 5. The diffractor is located at the x-coordinate 3000 meter. From the figure it is apparent that the fastest time, i.e., the time between diffractor location and its surface projection (red cross), is the vertical one and also the diffraction response is symmetrical to the vertical ray slice. Figure 1(b) displays the top view of the diffraction response for the dame geological medium with TTI anisotropy. The tilt is 45 degree, ϵ is 0.24, and δ is 0.13. From the figure it is apparent that the fastest time is not the vertical time anymore and the diffraction response becomes asymmetrical with larger offset.

Although there exists no analytical solution of the diffraction response in anisotropic media one can approximate it, e.g., by a traveltime expression derived by Alkhalifah and Tsvankin (1995) which is based on a non-hyperbolic reflection response. Their approximation represents an extension of the conventional isotropic DSR equation with an additional fourth-order term. This term depends on an additional parameter, η, which steers the non-hyperbolic part of the moveout. Moreover, their diffraction response is assumed to be symmetrical with respect to the time along the vertical ray which is considered to be the fastest

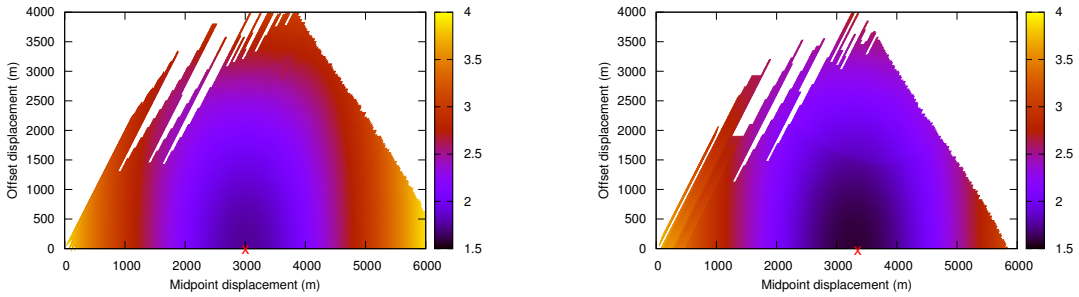

(a) **(b)**

Figure 1: (a) A top view of the diffraction response in an isotropic medium for a model shown in Figure 5. The diffractor is located at the x-coordinate 3000 meter. The diffractor surface projection coincides with the location where the fastest ray arrives (red cross). (b) A top view of the diffraction response in an anisotropic medium for the same model. The diffractor surface projection does not coincide with the location where the fastest ray arrives (red cross).

one (see, e.g., Figure 1 in Alkhalifah, 2000). However, this traveltime approximation is derived for media with a weak polar anisotropy and, hence, not applicable for strong and for general anisotropy. Figure 1(b) shows, however, that the apex of the diffraction response does not coincide with the subsurface projection of the diffractor location, i.e., the diffraction apex is laterally shifted. This feature is called *apex shift* in the following. This shift should be taken into account if we want to properly describe the diffraction response.

In this paper we consider a general anisotropic medium and propose to expand the ray velocity in a Taylor series. In the 2D case, this leads to a parameterization of the diffraction response with four parameters, namely the emergence angle of the fastest ray emanated from the diffractor, the ray velocity along this ray, and first and second-order derivatives of the ray velocity with respect to its angle. The four parameters of the diffraction response are required to describe the prestack diffraction response in the vicinity of the fastest ray for a general anisotropic 2D medium. Also, we show that for weak polar anisotropy with vertical symmetry the diffraction traveltime can be described by the ray velocity and the Thomsen parameter δ.

THEORY

We consider a general anisotropic homogeneous medium with the geometry shown in Figure 2. The position of a diffractor in the subsurface is given by x and z. x_0 is the location on the measurement surface where the fastest ray arrives and x_{sp} identifies the surface projection of the diffractor. x_1 and x_2 are the horizontal coordinates of source and receiver. The traveltime between the collocated source and receiver, i.e., from $(x_1, z = 0)$ via (x, z) to $(x_2, z = 0)$ can be calculated by applying Pythagorean theorem as

$$t = \frac{\sqrt{(x_{sp} - x_1)^2 + z^2}}{\nu(\varphi_1)} + \frac{\sqrt{(x_2 - x_{sp})^2 + z^2}}{\nu(\varphi_2)}\,, \tag{1}$$

where $\nu(\varphi_1), \nu(\varphi_2)$ are the ray velocities and φ_1, φ_2 angles as defined in Figure 2. Equation 1 represents the anisotropic DSR equation. Note that the ray velocity varies for different angles or offsets. To eliminate the angle dependency, we expand the ray velocity into a Taylor series in the vicinity of the fastest ray with respect to its angle.

The ray velocities along both rays are

$$\nu(\varphi_i) \approx \nu_0(1 + A(\varphi_i - \varphi_0) + B(\varphi_i - \varphi_0)^2), \quad (i = 1, 2)\,, \tag{2}$$

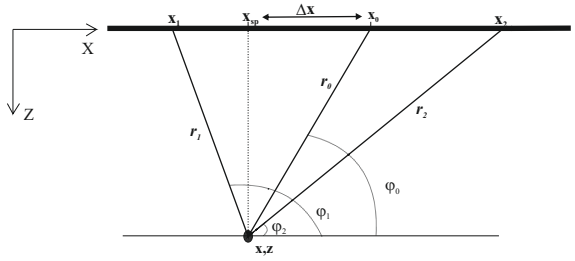

Figure 2: Geometry for a 2D general anisotropic medium.

where

$$\nu(\varphi_0) = \nu_0, \quad A = \frac{1}{\nu_0}\left.\frac{\partial \nu}{\partial \varphi}\right|_{\varphi_0}, \quad \text{and} \quad B = \frac{1}{2\nu_0}\left.\frac{\partial^2 \nu}{\partial \varphi^2}\right|_{\varphi_0}. \tag{3}$$

Here $\nu_0 = \nu(\varphi_0)$ is the ray velocity along the fastest ray. Substituting the ray velocities into the anisotropic DSR equation given by equation 1 yields

$$t = \frac{\sqrt{(x_{sp} - x_1)^2 + z^2}}{\nu_0(1 + A(\varphi_1 - \varphi_0) + B(\varphi_1 - \varphi_0)^2)} + \frac{\sqrt{(x_2 - x_{sp})^2 + z^2}}{\nu_0(1 + A(\varphi_2 - \varphi_0) + B(\varphi_2 - \varphi_0)^2)}. \tag{4}$$

This approximation depends on the surface projection of the diffractor $(x_{sp}, z = 0)$, the coordinates of the source and receiver $(x_1, z = 0)$ and $(x_2, z = 0)$, first and second-order derivatives of the ray velocity with respect to the ray angle (i.e., A and B), angle variations (i.e., $\varphi - \varphi_0$), the ray velocity along the fastest ray ν_0, and the depth coordinate z.

Note, that equation 4 directly depends on the angles. In appendix A we derive the equation 4 in midpoint-offset coordinates to make it consistent with common processing workflows. The midpoint-offset equation reads as

$$\begin{aligned} t = &\left(1 + A\frac{(m-h)\sin\varphi_0}{r_1} + (A^2 - B)\frac{(m-h)^2\sin^2\varphi_0}{r_1^2}\right) \\ &\times\sqrt{\frac{t_0^2}{4} + \frac{(m-h)^2}{\nu_0^2} + \frac{(m-h)t_0\cos\varphi_0}{\nu_0}} \\ &+\left(1 - A\frac{(m+h)\sin\varphi_0}{r_2} + (A^2 - B)\frac{(m+h)^2\sin^2\varphi_0}{r_2^2}\right) \\ &\times\sqrt{\frac{t_0^2}{4} + \frac{(m+h)^2}{\nu_0^2} + \frac{(m+h)\cos\varphi_0}{\nu_0}}, \end{aligned} \tag{5}$$

and is valid for a general 2D anisotropic medium and moderate offsets.

The transition from homogeneous to heterogeneous anisotropic medium is very similar to other cases (CMP operator, isotropic DSR operator). All medium parameters become "effective parameters". For anisotropy this is inherently frequency dependent, however, this is a different issue. If you have several diffractors at different depth, it is possible to determine interval parameters out off the effective parameters.

Because of the 3-D nature of the problem and the "point characteristics" of the diffractor it is not an easy task. It is very attractive though since it is applied post-stack and the illumination of diffractions is far superior to reflections.

Next, we discuss three special cases.

Isotropic homogeneous media

For an isotropic homogeneous medium, the first and second-order derivatives are equal to zero and the ray velocity coincides with the phase velocity. Also the fastest ray coincides with the vertical ray so that the angle of emergence, φ_0, equals $\frac{\pi}{2}$. In this case, the new traveltime approximation given by equation 5 simplifies to

$$t = \sqrt{\frac{t_0^2}{4} + \frac{(m-h)^2}{v^2}} + \sqrt{\frac{t_0^2}{4} + \frac{(m+h)^2}{v^2}}\,, \tag{6}$$

where v is the phase velocity. The obtained expression is identical to the conventional DSR equation.

Isotropic strongly heterogeneous media

In this case the first and second-order derivatives equal zero and the ray velocity coincides with the phase velocity. However, the fastest ray may not coincide with the vertical ray because of the inhomogeneities. The diffraction traveltime approximation given by equation 5 simplifies to

$$t = \sqrt{\frac{t_0^2}{4} + \frac{(m-h)^2}{v^2} - 2(m-h)t_0p_0} + \sqrt{\frac{t_0^2}{4} + \frac{(m+h)^2}{v^2} + 2(m+h)t_0p_0}\,, \tag{7}$$

where p_0 is a ray parameter given by

$$p_0 = \frac{\cos\varphi_0}{\nu_0}\,. \tag{8}$$

The inhomogeneity is hidden in the third term inside the square roots which we interpret as a lateral shift of the diffraction apex with respect to the diffractor location.

Weak anisotropic media with vertical polar symmetry

In the case of weak VTI, the fastest ray coincides with the vertical ray, i.e. $\varphi_0 = \frac{\pi}{2}$. The diffraction traveltime given by Equation 23 simplifies to

$$\begin{aligned} t = &\sqrt{\frac{t_0^2}{4} + \frac{(m-h)^2}{\nu_0^2}} \left(1 + A\frac{m-h}{\sqrt{\frac{t_0^2\nu_0^2}{4} + (m-h)^2}} + (A^2 - B)\frac{(m-h)^2}{\frac{t_0^2\nu_0^2}{4} + (m-h)^2}\right) + \\ &\sqrt{\frac{t_0^2}{4} + \frac{(m+h)^2}{\nu_0^2}} \left(1 - A\frac{m+h}{\sqrt{\frac{t_0^2\nu_0^2}{4} + (m+h)^2}} + (A^2 - B)\frac{(m+h)^2}{\frac{t_0^2\nu_0^2}{4} + (m+h)^2}\right)\,. \end{aligned} \tag{9}$$

Furthermore, for weak VTI media the following relations are valid (see, e.g., Tsvankin, 2001)

$$A = \frac{1}{\nu_0}\frac{\partial\nu}{\partial\varphi} = 0 \quad \text{and} \quad B = \frac{1}{2\nu_0}\frac{\partial^2\nu}{\partial\varphi^2} = \delta\,, \tag{10}$$

where δ is the Thomsen parameter. This leads to

$$t = \left(1 - \frac{\delta(m-h)^2}{\frac{t_0^2\nu_0^2}{4} + (m-h)^2}\right)\sqrt{\frac{t_0^2}{4} + \frac{(m-h)^2}{\nu_0^2}} + \left(1 - \frac{\delta(m+h)^2}{\frac{t_0^2\nu_0^2}{4} + (m+h)^2}\right)\sqrt{\frac{t_0^2}{4} + \frac{(m+h)^2}{\nu_0^2}}\,. \tag{11}$$

Note, the weak VTI approximation directly depends on δ which allows to invert surface seismic data for δ.

NUMERICAL EXAMPLES

We consider polar symmetry with vertical and 60 degree tilted symmetry axes. The anisotropy itself changes from weak to moderate. For VTI media we compare the new traveltime approximation and the approximation of Alkhalifah and Tsvankin (1995) with the exact traveltimes for a point diffractor located at the depth of 2 km. We compute the exact traveltimes solving the Christoffel equation. For TTI, media we compare the new approximation, approximations of Pech et al. (2003) and Grechka and Pech (2006) with the exact traveltimes.

Figure 3(a) shows traveltime plots for a weak VTI medium with $\epsilon = 0.03$ and $\delta = 0.045$. The vertical qP-velocity is 3810 m/s. The red crosses represent the new approximation, the black line represent the exact traveltimes, and the blue points represents the traveltimes computed by Alkhalifah's approximation. We observe that for the weak VTI both approximations fit the exact traveltimes almost perfectly. Figure 3(b) shows traveltime plots for a VTI medium with $\epsilon = 0.195$ and $\delta = 0.175$. The vertical qP-velocity is 2106 m/s. Both approximations fit the exact traveltimes considerable but worse than in the previous case. Figure 3(c) shows the traveltime comparison for a medium with even stronger VTI anisotropy where $\epsilon = 0.223$ and $\delta = 0.204$. The vertical qP-velocity is 2870 m/s. Again, both approximations fit the exact traveltimes considerable. We also observe that for larger offsets Alkhalifah's approximation fits the exact traveltimes slightly better than the new approximation. We explain this behavior by the following reasons. Because of the Taylor expansion, the new approximation depends only on Thomsen parameter δ which steers traveltime moveout near to the fastest ray. Parameter ϵ affects more the reflection moveout at larger offsets. To improve the accuracy at larger offsets we can include higher order terms in the Taylor series (see equation 2). Alkhalifah's approximation accounts for both Thomsen parameters δ and ϵ through the parameter $\eta = \epsilon - \delta$. However, Alkhalifah's approximation is sensitive to the parameter η and in all previous examples the parameter η is small. Figure 3(d) shows the behavior of the different approximations when the parameter η is large. We keep the vertical qP-velocity and δ as in Figure 3(c) and only change the sign of δ. In this case $\eta = 0.427$ and we observe that Alkhalifah's approximation is not accurate also at near offsets.

Figure 4(a) shows traveltime plots for a weak TTI medium with $\epsilon = 0.065$ and $\delta = 0.059$. The tilt is 60 degree and the vertical qP-velocity is 3.383 km/s. The point diffractor is located at the depth of 2 km. The red crosses represent the new approximation, the black line represents the exact traveltimes, the purple points represents the Pech's approximations and the blue dotted line represents the Grechka's and Pech's approximation. The new approximation fits the exact traveltimes almost perfectly. Examining Figure 4(b), 4(c), and 4(d) we observe that the new approximation is better for TTI media than for the VTI examples specially at larger offsets. We explain this behavior with the fact that the TTI approximation depends on two anisotropic parameters which account for both near-offset and far-offset anisotropic effects. In appendix C, TTI anisotropic stacking parameters are expressed by Thomsen parameters ϵ and δ.

SYNTHETIC DATA EXAMPLE

We use the new traveltime approximation as the prestack operator applied to a synthetic data example to demonstrate whether it will focus diffractions. The model consist of two layers and a small sphere acting as a diffracting object (Figure 5). The vertical velocity within the layers is constant. In the first layer it is 1500 m/s, and in the second layer 2000 m/s. The sphere has a radius of 100 meters. We used NORSAR ray tracer to generate synthetic seismograms using a Ricker-wavelet with a central peak frequency of 20 Hz, i.e., the prevailing wavelength is about 100 m in the second layer. Figure 7(a) shows the ZO section.

We use the ZO section and the stacking operator given by Equation 11 to estimate anisotropic parameters δ and velocity ν_0. For this purpose, we perform a simultaneous search for δ and ν_0. Figure 6(a) shows the coherence map after the bispectral analysis. We observe a very good focusing with high coherence. For a comparison Figure 6(b) shows the coherence map after conventional one-parameter analysis. As expected, we observe lower coherence values. With the estimated anisotropic parameters we then perform the prestack time migration.

Figure 7(b) shows the migrated section when using the new approximation as the PreSTM operator. The maximum offset to be migrated is 4000 meters. The migration midpoint aperture is 4000 meters and no filtering is applied to the time-migrated result. We observe a very high focusing of the diffraction.

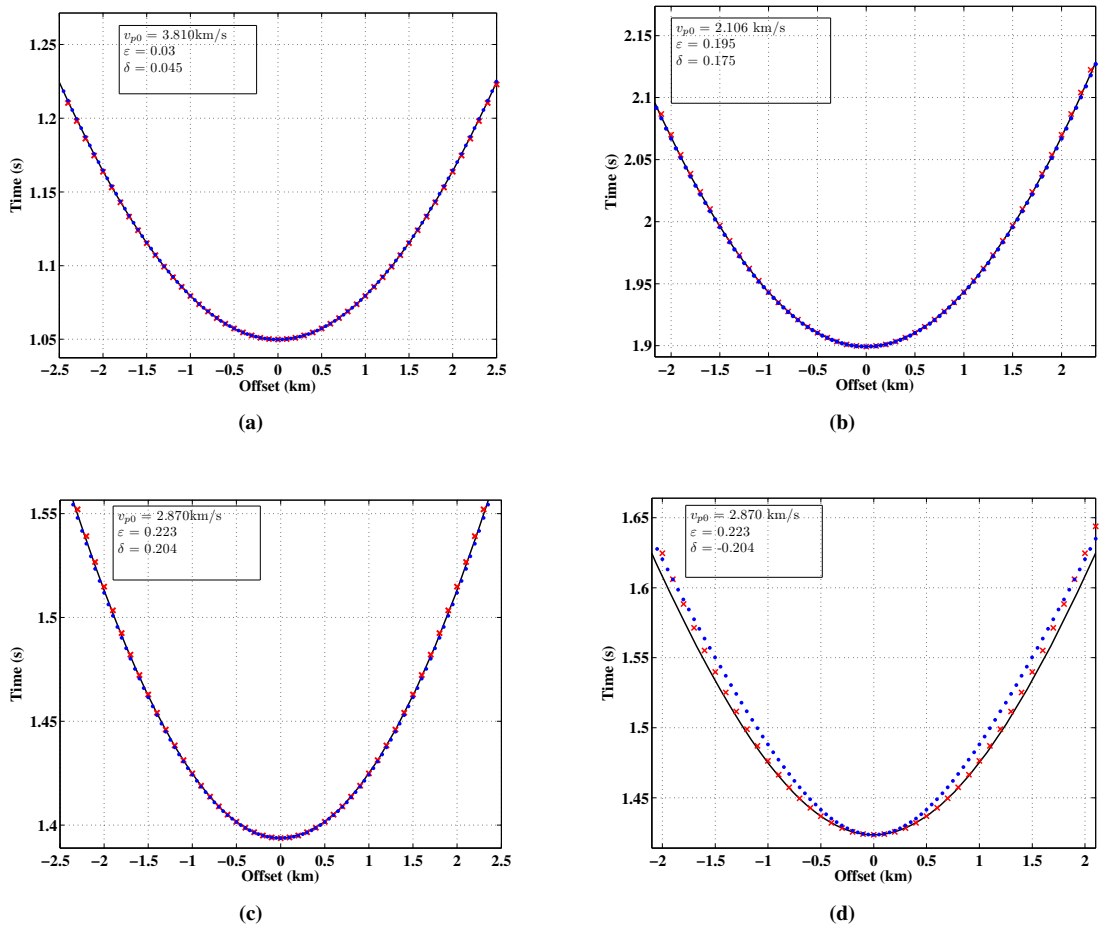

Figure 3: Comparison of traveltimes for homogeneous VTI media computed by solving Christoffel equation (black line), by the new approximation (red crosses) and by Alkhalifah's approximation (blue points). The point diffractor is located at 2 km depth. v_{p0} represents the vertical qP-velocity.

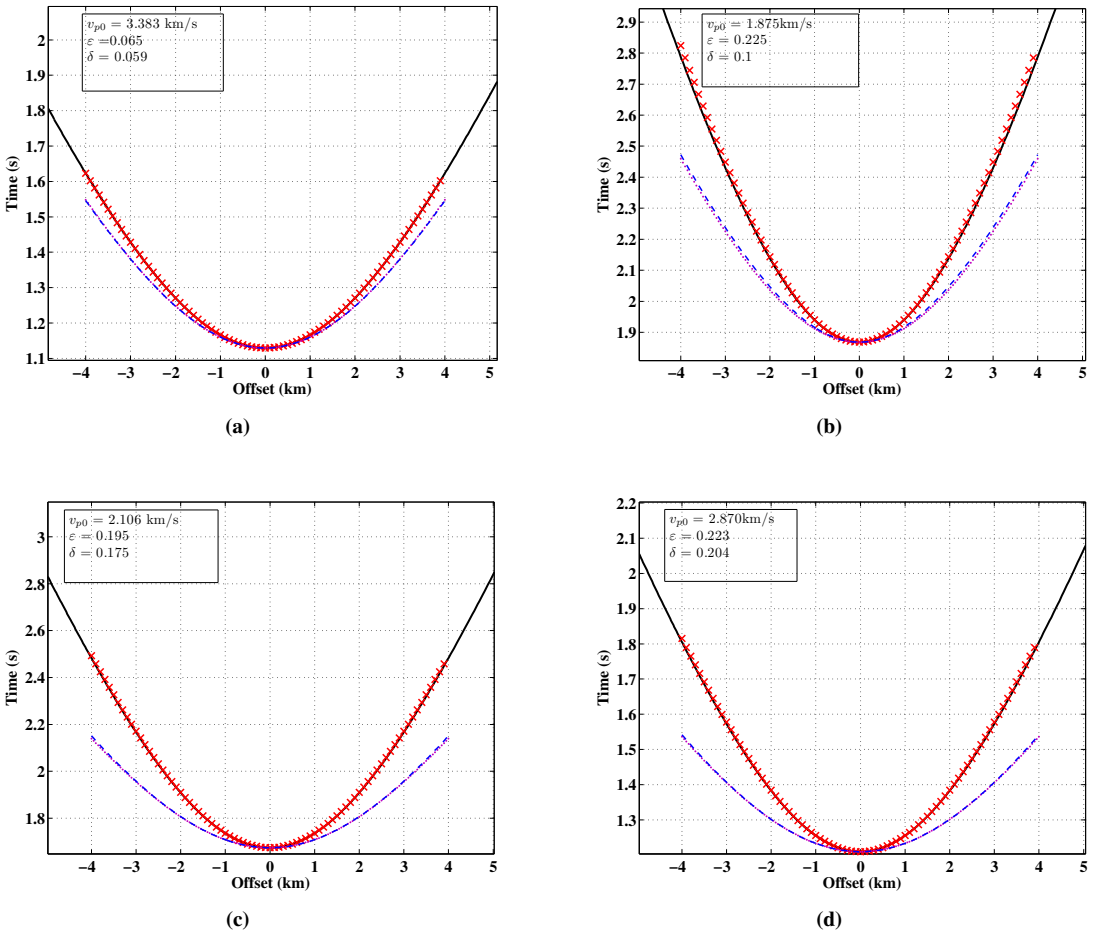

Figure 4: Comparison of traveltimes in TTI media. The point diffractor is located at 2 km depth. The axis of symmetry is rotated by 60^o. The crosses represent the new approximation, the line represents the exact traveltimes, the points represent the Pech's approximations and the dotted line represent the Grechka's and Pech's approximation. v_{p0} represents the vertical qP-velocity.

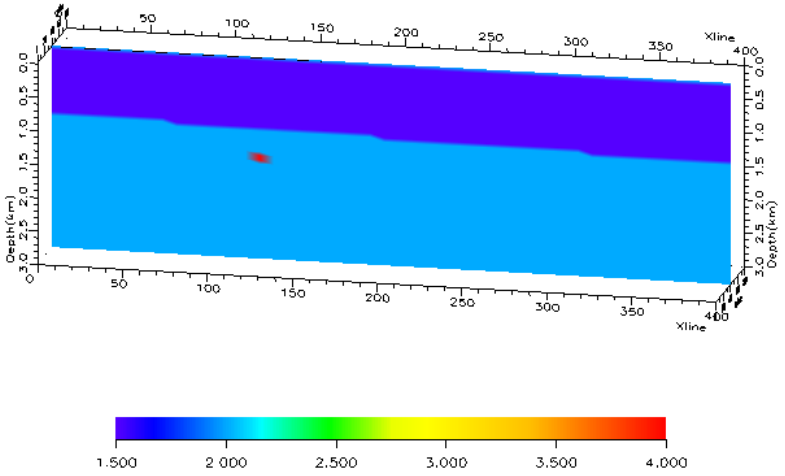

Figure 5: Geological model consisting of two homogeneous VTI layers and a diffracting spherical object of 100 m radius. The vertical velocity in the fist layer is 1500 m/s, in the second layer 2000 m/s. Thomsen parameters in both layers are $\epsilon = 0.24$ and $\delta = 0.13$. The symmetry axis is vertical.

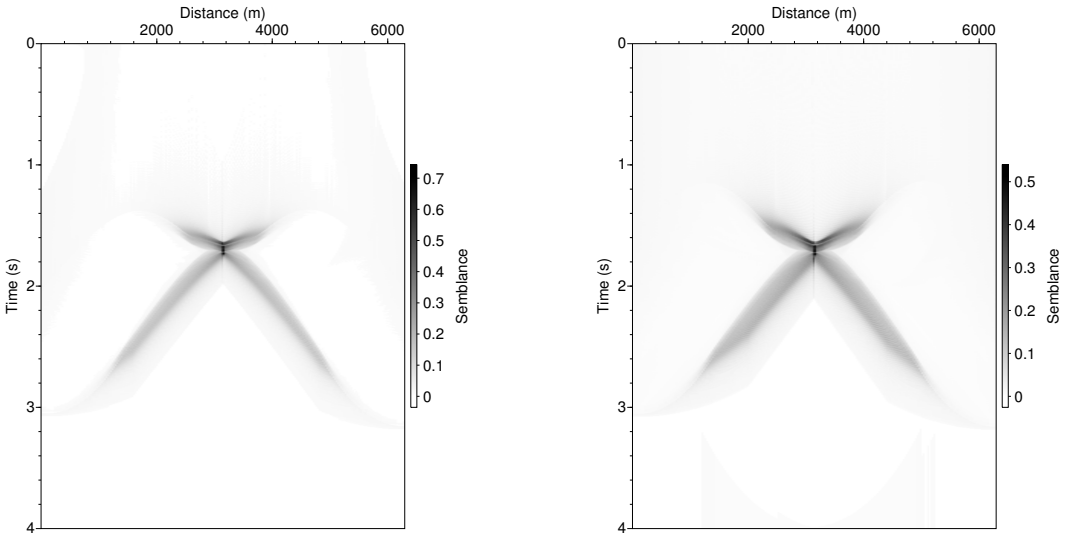

(a) **(b)**

Figure 6: (a) Coherence map after bispectral analysis for δ and velocity ν_0. We observe a good focusing with high coherence values. (b) Coherence map after monospectral analysis for velocity v. As expected, we observe lower coherence values.

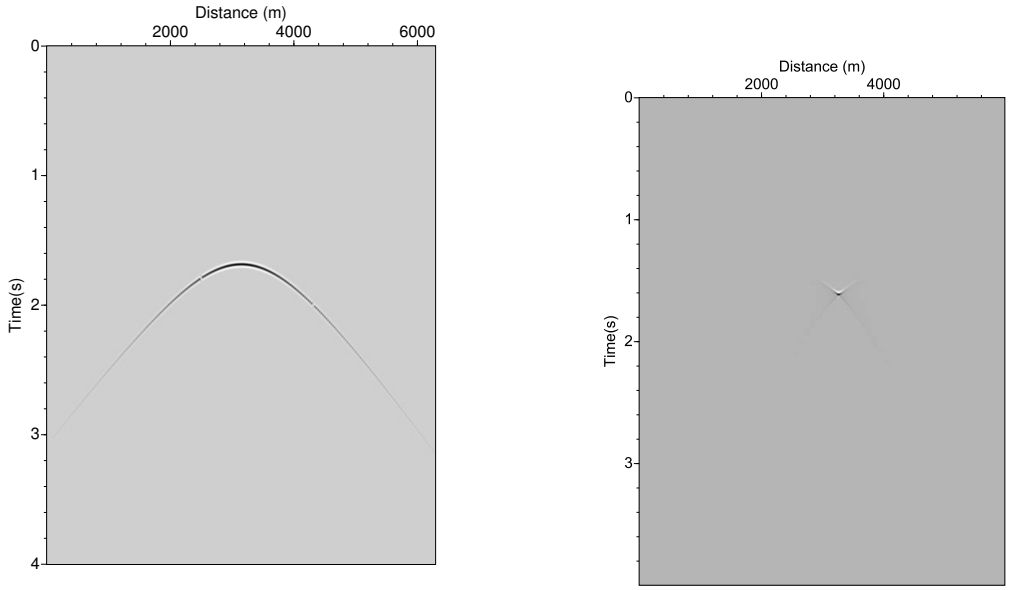

(a) **(b)**

Figure 7: (a) Zero offset section for the synthetic model obtained with NORSAR ray-tracing package. We used a Ricker-wavelet with a prevailing frequency of 20 Hz. Response from the first reflector was muted. (b) PreSTM result using the new diffraction traveltime approximation as the PreSTM operator. The maximum offset is 4000 meters.

CONCLUSIONS

We presented a new traveltime approximation for the diffraction response. We considered general anisotropic media and proposed to expand the ray velocity in a Taylor series which leads to a good performance of the operator for short offsets. In the 2D case, this leads to a parameterization of the diffraction response with four parameters: the emergence angle of the fastest ray, the ray velocity along this ray and first and second-order derivatives of the ray velocity with respect to its angle. For weak anisotropy these attributes can be calculated to anisotropic parameters.

Numerical and synthetic examples show that the proposed traveltime approximation fits the diffraction response considerable well independent from the anisotropy type. Using the new approximation as the time migration operator leads to a highly focused diffraction image.

ACKNOWLEDGMENTS

The authors would like to thank the sponsors of WIT consortium for their support. Sergius Dell and Dirk Gajewski are grateful to the ASG Hamburg for discussions. Boris Kashtan and Anna Pronevich would like to thank the Earth Physics Department of St. Petersburg State University, particularly Vladimir Troyan for continuous support. We also thank NORSAR Innovation AS for kindly permission to use ray-tracer.

REFERENCES

Alkhalifah, T. (2000). The offset-midpoint traveltime pyramid in transversely isotropic media. *Geophysics*, 65(4):1316–1325.

Alkhalifah, T. and Tsvankin, I. (1995). Velocity analysis for transversely isotropic media. *Geophysics*, 60:1550–1566.

Dell, S. and Gajewski, D. (2011). Common-reflection-surface-based workflow for diffraction imaging. *Geophysics*, 76(5):S187;doi:10.1190/geo2010–0229.1.

Dell, S. and Gajewski, D. (2012). 3D velocity model building based on diffractions. In *Saint Petersburg 2012. International Conference and Exhibition*, page A040. Extended Abstracts.

Dell, S., Kashtan, B., and Gajewski, D. (2012). Diffraction traveltime approximation for an arbitrary anisotropic medium: A case study. In *74th Conference and Technical Exhibition, EAGE*, page P365. Extended Abstracts.

Grechka, V. and Pech, A. (2006). Quartic reflection moveout in a weakly anisotropic dipping layer. *Geophysics*, 71:D1–D13.

Khaidukov, V., Landa, E., and Moser, T. J. (2004). Diffraction imaging by focusing-defocusing: An outlook on seismic superresolution. *Geophysics*, 69:1478–1490.

Landa, E. and Keydar, S. (1997). Seismic monitoring of diffraction images for detection of local heterogeneities. *Geophysics*, 63:1093–1100.

Pech, A., Tsvankin, I., and Grechka, V. (2003). Quartic moveout coefficient: 3D description and application to tilted TI media. *Geophysics*, 68:1600–1610.

Reshef, M. and Landa, E. (2009). Post-stack velocity analysis in the dip-angle domain using diffractions. *Geophysical Prospecting*, 57:811–821.

Tsvankin, I. (2001). *Seismic signatures and analysis of reflection data in anisotropic media*. Pergamon.

APPENDIX A

Here we derive the diffraction response given by equation in midpoint-offset coordinates to make it consistent with common processing workflows. For this purpose, we express x and z coordinates with respect to the zero-offset (ZO) traveltime. We calculate the ZO traveltime using Pythagorean theorem, i.e.,

$$t_0 = \frac{2}{\nu_0}\sqrt{(x_{sp}-x_0)^2+z^2}\,. \tag{12}$$

We denote the apex shift as

$$\Delta x \equiv x_0 - x_{sp}\,. \tag{13}$$

Then, we rewrite the terms $(x_{sp}-x_1)^2$ and $(x_2-x_{sp})^2$ as

$$(x_{sp}-x_1)^2 = ((x_0-x_1)-(x_0-x_{sp}))^2 = ((x_0-x_1)-\Delta x)^2 = (x_0-x_1)^2+\Delta x^2-2\Delta x(x_0-x_1)\,, \tag{14}$$

$$(x_2-x_{sp})^2 = ((x_2-x_0)+(x_0-x_{sp}))^2 = ((x_2-x_0)-\Delta x)^2 = (x_2-x_0)^2+\Delta x^2+2\Delta x(x_2-x_0)\,, \tag{15}$$

We substitute equations 2-3 into the DSR traveltime approximation of equation 4 and obtain

$$t = \frac{1}{\nu(\varphi_1)}\sqrt{(x_0-x_1)^2-2(x_0-x_1)\Delta x+\frac{t_0^2\nu_0^2}{4}}+\frac{1}{\nu(\varphi_2)}\sqrt{(x_2-x_0)^2+2(x_2-x_0)\Delta x+\frac{t_0^2\nu_0^2}{4}}\,. \tag{16}$$

Taking ν_0 out of the square root leads to

$$t = \frac{\nu_0}{\nu(\varphi_1)}\sqrt{\frac{t_0^2}{4}+\frac{(x_0-x_1)^2}{\nu_0^2}-\frac{2(x_0-x_1)\Delta x}{\nu_0^2}}+\frac{\nu_0}{\nu(\varphi_2)}\sqrt{\frac{t_0^2}{4}+\frac{(x_2-x_0)^2}{\nu_0^2}+\frac{2(x_2-x_0)\Delta x}{\nu_0^2}}\,. \tag{17}$$

Inverting the ray velocities given by equation 2 as

$$\frac{1}{\nu(\varphi_i)} \approx \frac{1}{\nu_0}(1-A(\varphi_i-\varphi_0)+(A^2-B)(\varphi_i-\varphi_0)^2), \quad (i=1,2)\,, \tag{18}$$

and substituting them into equation 17 gives

$$t = \sqrt{\frac{t_0^2}{4} + \frac{(x_0 - x_1)^2}{\nu_0^2} - \frac{2(x_0 - x_1)\Delta x}{\nu_0^2}} \left(1 + A(\varphi_1 - \varphi_0) + (A^2 - B)(\varphi_1 - \varphi_0)^2\right) + \sqrt{\frac{t_0^2}{4} + \frac{(x_2 - x_0)^2}{\nu_0^2} + \frac{2(x_2 - x_0)\Delta x}{\nu_0^2}} \left(1 - A(\varphi_2 - \varphi_0) + (A^2 - B)(\varphi_2 - \varphi_0)^2\right) . \quad (19)$$

In appendix B we show how to remove the angle dependency by a sine approximation of the angle, i.e.,

$$\varphi_i - \varphi_0 \approx (-1)^i \frac{(m \mp h)\sin\varphi_0}{r_i}, \quad (i = 1, 2) , \quad (20)$$

where r_1, r_2 are the distances from the diffractor to the source and receiver, respectively, and h is the half offset coordinate. We express the shift Δx, and depth z as

$$x_0 - x_{sp} = \frac{t_0\nu_0}{2}\cos\varphi_0 , \quad z = \frac{t_0\nu_0}{2}\sin\varphi_0 , \quad (21)$$

and x_1, x_2 coordinates in midpoint-offset coordinates as

$$x_2 = x_m + h , \quad x_1 = x_m - h . \quad (22)$$

Using expressions 21 and 22 into equation 19, yields

$$\begin{aligned} t = &\left(1 + A\frac{(m-h)\sin\varphi_0}{r_1} + (A^2 - B)\frac{(m-h)^2\sin^2\varphi_0}{r_1^2}\right) \\ &\times\sqrt{\frac{t_0^2}{4} + \frac{(m-h)^2}{\nu_0^2} + \frac{(m-h)t_0\cos\varphi_0}{\nu_0}} \\ &+ \left(1 - A\frac{(m+h)\sin\varphi_0}{r_2} + (A^2 - B)\frac{(m+h)^2\sin^2\varphi_0}{r_2^2}\right) \\ &\times\sqrt{\frac{t_0^2}{4} + \frac{(m+h)^2}{\nu_0^2} + \frac{(m+h)\cos\varphi_0}{\nu_0}}, \end{aligned} \quad (23)$$

where $m = x_m - x_0$ is the midpoint displacement. Equation 23 represents the diffraction response approximate which is valid for a general 2D anisotropic medium and moderate angles.

APPENDIX B

To exclude the angle dependency on the traveltime expression we propose to use a sine approximation. For small angles the sine is equal to its argument, i.e.,

$$\sin x \approx x . \quad (24)$$

Alternatively, a tangent approximation can be applied, as described in (Dell et al., 2012). Using

$$\sin(\varphi_i - \varphi_0) = \sin\varphi_i\cos\varphi_0 - \sin\varphi_0\cos\varphi_i, \quad i = 1, 2 , \quad (25)$$

yields

$$\varphi_i - \varphi_0 \approx \frac{z}{r_i}\cos\varphi_0 - \frac{x_i - x}{r_i}\sin\varphi_0, \quad i = 1, 2 . \quad (26)$$

r_1 and r_2 are the distances from diffractor to the source and receiver determined as

$$r_1 = \sqrt{\frac{t_0^2\nu_0^2}{4} + (m-h)^2 + t_0\nu_0(m-h)\cos\varphi_0} \quad \text{and} \quad r_2 = \sqrt{\frac{t_0^2\nu_0^2}{4} + (m+h)^2 + t_0\nu_0(m+h)\cos\varphi_0} \quad (27)$$

Making use of equation 21 yields

$$\varphi_1 - \varphi_0 \approx -\frac{(m-h)\sin\varphi_0}{r_1} \quad \text{and} \quad \varphi_2 - \varphi_0 \approx \frac{(m+h)\sin\varphi_0}{r_2} . \quad (28)$$

APPENDIX C

Group velocity in weak TI media can be approximated (see Tsvankin, 2001) as

$$\nu(\varphi^*) = \nu_0(1 + \delta \sin^2 \varphi^* \cos^2 \varphi^* + \epsilon \sin^4 \varphi^*)\,, \tag{29}$$

where the ϵ and δ are Thomsen parameters and φ^* is the difference between the angel φ and the title angle ψ (i.e., $\varphi^* = \varphi - \psi$).

The first and second-order derivatives of the ray velocity with respect to the angle φ^* are calculated as

$$\begin{aligned} \frac{\partial \nu}{\partial \varphi^*} &= \nu_0 \sin 2\varphi^* (\delta \cos 2\varphi^* + 2\epsilon \sin^2 \varphi^*)\,, \\ \frac{\partial^2 \nu}{\partial (\varphi^*)^2} &= 2\nu_0 \left[\delta \cos 4\varphi^* + 2\epsilon \sin^2 \varphi^* (2\cos^2 \varphi^* + 2\cos 2\varphi^*)\right]\,. \end{aligned} \tag{30}$$

Substituting the expressions above in equation 3 yields the anisotropic stacking parameters

$$\begin{aligned} A &= \sin 2\varphi^* (\delta \cos 2\varphi^* + 2\epsilon \sin^2 \varphi^*)\,, \\ B &= \delta \cos 4\varphi^* + 2\epsilon \sin^2 \varphi^* (2\cos^2 \varphi^* + 2\cos 2\varphi^*)\,. \end{aligned} \tag{31}$$